Journal of Materials Chemistry B

PAPER

View Article Online
View Journal | View Issue

Cite this: J. Mater. Chem. B, 2018, 6, 7060

Construction of a novel near-infrared fluorescent probe with multiple fluorescence emission and its application for SO_2 derivative detection in cells and living zebrafish†

Keyin Liu, *[ab] Yunling Chen,[a] Hui Sun,[c] Shoujuan Wang[a] and Fangong Kong*[a]

Received 2nd August 2018,
Accepted 5th October 2018

DOI: 10.1039/c8tb02030b

rsc.li/materials-b

Sulfur dioxide (SO_2) in biological systems is an important gaseous signal molecule and plays important roles in physiological activities. It can be endogenously produced by enzymes in mitochondria during oxidation of sulphur-containing molecules. Thus, the development of probes for sulfur dioxide detection in biological environment is necessary. Here, a new near-infrared fluorescent probe (**Rh-TPA**) with multiple fluorescence emission was constructed and applied for SO_2 derivative detection. **Rh-TPA** was constructed *via* conjugation of a rhodamine analogue with a triphenylamine group. **Rh-TPA** exhibited a major emission peak at 740 nm and a shoulder peak at 810 nm. After interacting with SO_2 derivatives, the conjugated system dissociated into two smaller chromophores with two emission peaks (520 nm and 570 nm) in the visible region. The probe showed negligible cytotoxicity, as demonstrated by the MTT results. Biological imaging application experiments indicated that the probe can be used to image SO_2 derivatives in HeLa cells and living zebrafish.

Introduction

Sulfur dioxide (SO_2) is widely known as a key pollutant existing in the atmosphere, which is predominantly generated by consumption of fossil fuels, industry production and volcanic eruption for many decades.[1,2] Medical physiology studies have shown that long time exposure to SO_2 in the atmosphere or drinking water containing high concentrations of sulfite (SO_3^{2-}) or bisulfite (HSO_3^-) may lead to several serious diseases[3,4] such as respiratory illness, lung disorders, cancer, neurological disorders, and cardiovascular diseases.[2,5] Moreover, sulfur dioxide (SO_2) and its ionic hydrates (SO_3^{2-} or HSO_3^-) are very important chemical species that are widely applied in fine chemical, food and pharmaceutical industries.[3,6] However, excessive sulfite intake is harmful to human health, and the amount of sulfite as an additive must be under strict control. A recent study has demonstrated that SO_2 can be endogenously generated, and it plays a key role in physiological environment.[7] It can be endogenously produced by enzymes in mitochondria during oxidation of sulphur-containing molecules such as H_2S, cysteine and homocysteine.[8] Therefore, it is of great significance to develop a new method for SO_2 derivative detection in living organisms.

Many methods for SO_2 derivative detection have been developed in recent years, and they include electrochemical methods, chromatography, colorimetry, titration, and gas chromatography–mass spectrometry (GC–MS).[9–15] Among them, the fluorescence imaging technique is one of the most powerful methods for SO_2 detection in living organisms due to the advantages of noninvasive, real-time and *in situ* analysis.[16–19] Due to these advantages of fluorescence imaging, recently, several highly sensitive fluorescent probes for SO_2 detection have been reported based on modification of traditional dyes such as fluorescence,[20] coumarin,[21–24] and cyanine derivatives.[6,25–28] Some of the probes are based on the fluorescence turn-on/turn-off response towards SO_2, which may suffer from a comparatively low sensitivity or high fluorescence background. Compared with fluorescence turn-on/turn-off-type probes, ratiometric fluorescent probes can eliminate most of the interference by measuring the ratio change of fluorescence intensity at two different emission wavelengths.[22] Hence, the development of new fluorescent probes with multiple fluorescence emission is more beneficial for SO_2 derivative detection in complex biological samples.

Herein, we have reported a new strategy for the construction of a novel near-infrared fluorescent probe with multiple fluorescence emission. The probe for SO_2 derivatives was constructed

[a] Key Laboratory of Pulp and Paper Science and Technology of Ministry of Education, Qilu University of Technology (Shandong Academy of Sciences), Jinan, Shandong 250353, P. R. China. E-mail: keyinliu@163.com, kfg@qlu.edu.cn; Fax: +86-0531-89631168; Tel: +86-0531-89631168
[b] Institute of Fluorescent Probes for Biological Imaging, University of Jinan, Jinan, Shandong 250022, P. R. China
[c] Xuancheng product quality supervision and Inspection Institute, Xuan Cheng, An Hui, 242000, P. R. China

† Electronic supplementary information (ESI) available. See DOI: 10.1039/c8tb02030b

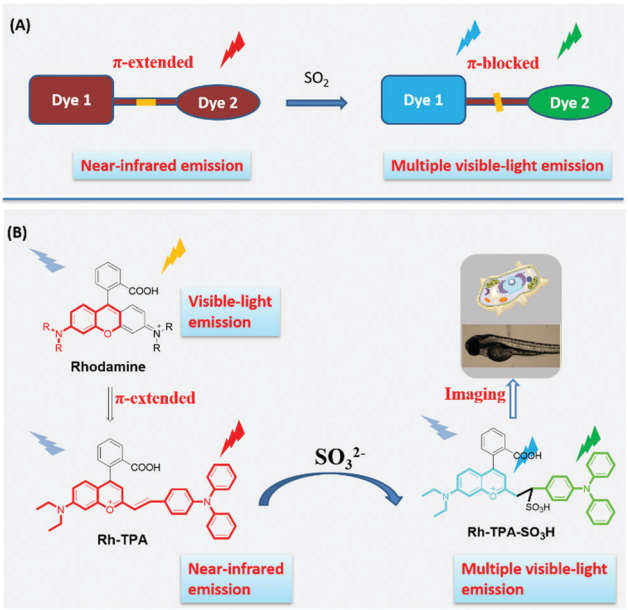

Fig. 1 (A) The general design strategy of a near-infrared fluorescent probe with multiple fluorescence emission and (B) the design and detection process of probe **Rh-TPA** toward SO_2 derivatives and potential application in bioimaging.

through connection of two chromophores with an active conjugated double bond (Fig. 1A). In the presence of SO_2, the conjugated double bond was broken, and the near-infrared fluorescent probe was separated into two distinct chromophores with emission at different wavelengths.

As an example, we have developed a novel near-infrared fluorescent dye (**Rh-TPA**) containing an active double bond in the dye skeleton (Fig. 1B). **Rh-TPA** was constructed through integration of a rhodamine-like structure (**2**) with 4-(diphenylamino)benzaldehyde (**3**) (Scheme 1). The triphenylamine group in **Rh-TPA** is a notable organic building block extensively used in dye construction with excellent fluorescence performance,[29] which may endow **Rh-TPA** with novel fluorescence properties. When interacting with SO_2 derivatives, the conjugated system in **Rh-TPA** dissociated into two smaller chromophores with two emission peaks in the visible region (Fig. 1). We envision that the near-infrared fluorescent probe **Rh-TPA** can detect SO_2 derivatives with clear fluorescence changes in both near infrared and visible-light regions.

Experimental

Reagents, materials and apparatus

Unless otherwise stated, all reagents were purchased from commercial suppliers and used without further purification. All solvents used were purified by standard methods prior to use. Silica gel thin layer chromatography (TLC) plates and silica gel (200–300 mesh) were purchased from Qingdao Ocean Ltd Co. All the reactions were monitored by silica thin layer chromatography (TLC), and the intermediates were purified by a silica gel column. ^{1}H NMR and ^{13}C NMR spectra were recorded on a

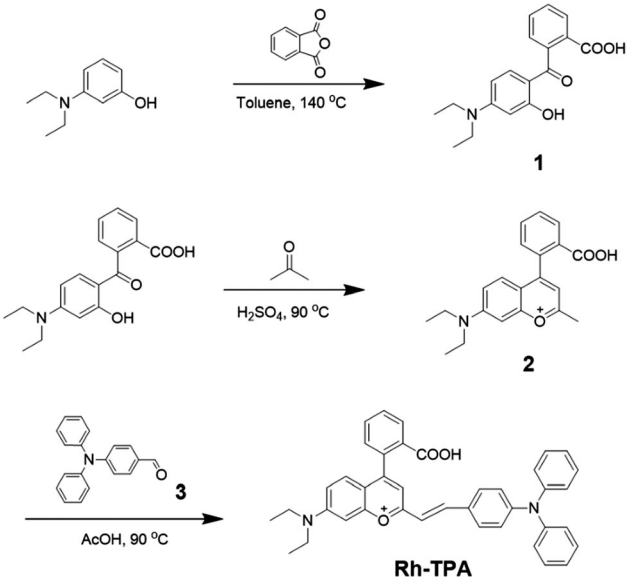

Scheme 1 The synthesis route of probe **Rh-TPA**.

Bruker Avance 400 NMR spectrometer. Double-distilled water was used in the solution preparation and measurement. The fluorescence spectra were measured on a Hitachi F4600 spectrofluorimeter (Hitachi High-Tech Science), and the UV-visible absorption spectra were recorded on a Shimadzu UV-2700 spectrophotometer (Shimadzu Suzhou instruments Mfg. Co, Ltd). All animal procedures for this study were approved by the Animal Ethical Experimentation Committee of Shandong University according to the requirements of the National Act on the use of experimental animals (China). Images of cells and zebrafish were collected on a Leica SP8 microscope instrument.

Synthesis procedures

Synthesis of 4-(2-carboxyphenyl)-7-(diethylamino)-2-methylchromenylium (2). Compound **1** and compound **2** were synthesized and characterized according to a previously reported method (Scheme 1).[30] Briefly, 3-(diethylamino)phenol and phthalic anhydride were refluxed in toluene solution for 12 h to acquire the crude product of compound **1**, which was purified by a silica gel column. Concentrated sulfuric acid (H_2SO_4), 10 mL, was carefully added into a 100 mL round bottom flask, and it was cooled to 0 °C by an ice bath. Then, 3 mL of acetone was added to the cooled H_2SO_4 solution dropwise, and compound **1** (0.6 g, 2.0 mmol) was added to the mixture in sequence. The mixture was stirred at 0 °C for 30 min and then heated to 90 °C by an oil bath for 4 h. The mixture was cooled to room temperature and then poured into 100 g crushed ice. Then, 2 mL of perchloric acid was added dropwise to the mixture while stirring. The crude product was obtained by filtration and then purified by a silica gel column by eluting with dichloromethane and methanol (v/v, 100/1–10/1). Compound **2** (0.21 g, 0.63 mmol) was obtained. Yield: 35%. ^{1}H NMR (400 MHz, MeOD-d_4) δ 8.30 (dd, J = 7.7, 1.1 Hz, 1H), 7.83 (dd, J = 7.5, 1.4 Hz, 1H), 7.78 (dd, J = 7.7, 1.4 Hz, 1H), 7.49–7.41

(m, 1H), 7.41–7.34 (m, 2H), 7.23–7.17 (m, 2H), 3.75 (q, J = 7.1 Hz, 4H), 2.81 (s, 3H), 1.34 (t, J = 7.1 Hz, 6H).

Synthesis of SO_2 probe Rh-TPA. Compound **2** (0.1 g, 0.3 mmol) and 4-(diphenylamino)benzaldehyde (0.09 g, 0.33 mmol) were added to a 50 mL round bottom flask; then, 10 mL of AcOH was added. The mixture was reacted at 90 °C under nitrogen protection for 6 hours, and the reaction was monitored by TLC. After compound **2** was consumed, the reaction mixture was cooled to room temperature and the solvent was removed using an evaporator. The crude product was further purified by a silica gel column by eluting with dichloromethane and methanol (v/v, 100/1–10/1). **Rh-TPA** (0.035 g, 0.06 mmol) was obtained. Yield 20%, ^{1}H NMR (400 MHz, MeOD-d_4) δ 8.10 (d, J = 15.8 Hz, 1H), 7.96 (d, J = 6.6 Hz, 1H), 7.65 (d, J = 8.9 Hz, 2H), 7.59 (dd, J = 6.1, 3.7 Hz, 2H), 7.47 (d, J = 9.5 Hz, 1H), 7.37 (m, 5H), 7.17 (m, 10H), 6.98 (d, J = 8.7 Hz, 2H), 3.69 (q, J = 7.0 Hz, 4H), 1.31 (t, J = 7.1 Hz, 6H). ^{13}C NMR (100 MHz, MeOD-d_4) δ 165.07, 162.63, 158.87, 155.40, 151.38, 146.32, 143.27, 134.55, 130.40, 130.27, 129.75, 129.46, 129.29, 129.22, 128.47, 127.44, 126.65, 125.87, 124.78, 120.05, 116.34, 116.23, 114.98, 113.52, 95.75, 45.38, 38.81, 33.35, 30.20, 28.69, 22.63, 11.36. HRMS (ESI) m/z calcd for $C_{40}H_{34}N_2O_3Na$ $[M-H+Na]^+$: 613.2462, found: 613.2426.

Cell culture and fluorescence imaging

HeLa cells were obtained from the Institute of Biochemistry and Cell Biology, Shanghai Institute of Biological Sciences (SIBS), Chinese Academy of Science. HeLa cells were cultured in Dulbecco's modified Eagle's medium (DMEM) containing 10% fetal bovine serum and antibiotics (100 units per mL penicillin and 100 μg mL^{-1} streptomycin) and maintained at 37 °C in an incubator atmosphere of 5% CO_2 and 95% air. A fresh stock solution of HeLa cells was seeded into glass bottom dishes with a density of about 1×10^{-5} cells per dish. The cells were then incubated at 37 °C in an incubator for 24 h before fluorescence imaging. In the experimental group, the cells were pre-treated with 50 μM of SO_3^{2-} for 20 min and then exposed to 10 μM of **Rh-TPA** for another 20 min at room temperature. In the control group, the cells were only exposed to 10 μM of **Rh-TPA** for 20 min before fluorescence imaging. The flow cytometry experiments were performed with a Moflo XDP (Beckman Coulter) instrument, red channel: λ_{ex} = 640 nm, filter: 750 ± 20 nm; green channel: λ_{ex} = 488 nm, filter: 550 ± 20 nm.

Zebrafish maintenance and imaging

The wild-type zebrafish were purchased from Nanjing Eze-Rinka Ltd Co. China, and all zebrafish experiments were performed fully according to the international ethics guidelines. Zebrafish were cultured at 28 °C and maintained at optimal breeding conditions on a 12 h light/12 h dark cycle. The embryos of zebrafish were transferred into glass dishes filled with E3 media (15 mM NaCl, 0.5 mM KCl, 1.0 mM $MgSO_4$, 1.0 mM $CaCl_2$, 0.15 mM KH_2PO_4, 0.05 mM Na_2HPO_4, 0.7 mM $NaHCO_3$; pH 7.5). For the fluorescence imaging experiments, 4-day-old larvae were transferred into a 96-well plate by a disposable transfer pipette in 1 mL of culture medium. In the experimental group, the larvae were pretreated with 50 μM of SO_3^{2-} for 20 min and then treated with 20 μM **Rh-TPA** for 30 min. In the control group, the larvae were only exposed to 20 μM of **Rh-TPA** for 30 min before fluorescence imaging.

Result and discussion

The spectral response of probe Rh-TPA towards SO_2 derivatives

The photophysical properties of the intermediates **2** and **3** and the SO_2 derivative probe **Rh-TPA** in solution were explored (Fig. S1–S4, ESI†). Interestingly, in the absorption spectra, **Rh-TPA** showed a maximum absorption peak at around 640 nm and a shoulder peak at 495 nm. In the fluorescence spectra, the probe showed an emission band at 740 nm and a shoulder peak at 810 nm (Fig. S3, ESI†). The fluorescence emission is probably due to the $\pi^* \rightarrow \pi$ electron transition in **Rh-TPA**.[31] Then, we investigated the spectral changes in **Rh-TPA** towards SO_2 derivatives. As shown in Fig. 2, in the absorption spectra, the absorption at 650 nm decreased sharply with the addition of SO_3^{2-}; meanwhile, a new absorption band emerged at 420 nm.

In accordance with the change in absorption spectra, a considerable fluorescence change was also observed in the emission spectra (Fig. 3). As shown in Fig. 3(a and b), with the concentration increase of an SO_2 derivative, a remarkable fluorescence turn-on was observed at both 520 nm and 570 nm. Synchronously, the emission peaks at 740 nm and 810 nm decreased sharply with the addition of SO_2 derivative with the fluorescence intensity change of nearly 10-fold (Fig. 3c and d). When evaluated by using the change in the ratiometric fluorescence intensity of the two emission peaks (F_{520}/F_{740}), up to 60-fold fluorescence enhancement was observed with the SO_2 to probe ratio change (Fig. 3e). The detection limit of **Rh-TPA** toward SO_2 derivatives was about 3.2×10^{-6} M, as calculated from the linear fit analysis (Fig. 3f). The time-dependent fluorescence change of **Rh-TPA** toward SO_2 derivatives was also measured. As shown by Fig. 4, the fluorescence at 520 nm increased steadily, whereas the fluorescence at 740 nm decreased over 80 min. The detection limit was lower than the allowed limit of additives in food industry; thus, the probe is suitable for SO_2 derivative detection in living animals.[5]

The fluorescence change mechanism was also proved by ^{1}H NMR and LC-MS analyses. As shown in ^{1}H NMR spectra (Fig. S5, ESI†), after the reaction with sulphite, the proton shifts

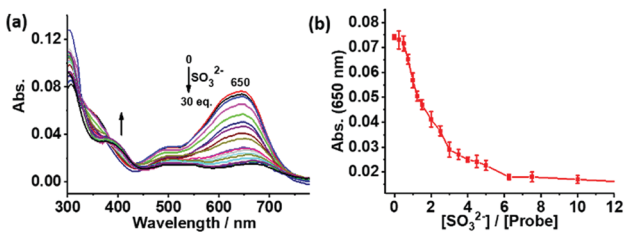

Fig. 2 The absorption spectra change of **Rh-TPA** titrated with SO_3^{2-}. (a) The absorption spectra change of 10 μM of **Rh-TPA** titrated with increasing concentrations of SO_3^{2-} in PBS (pH 7.4, 10 mM). (b) The absorption changes at 650 nm with the SO_3^{2-} to probe ratio increase. Error bars are ±SD, n = 3.

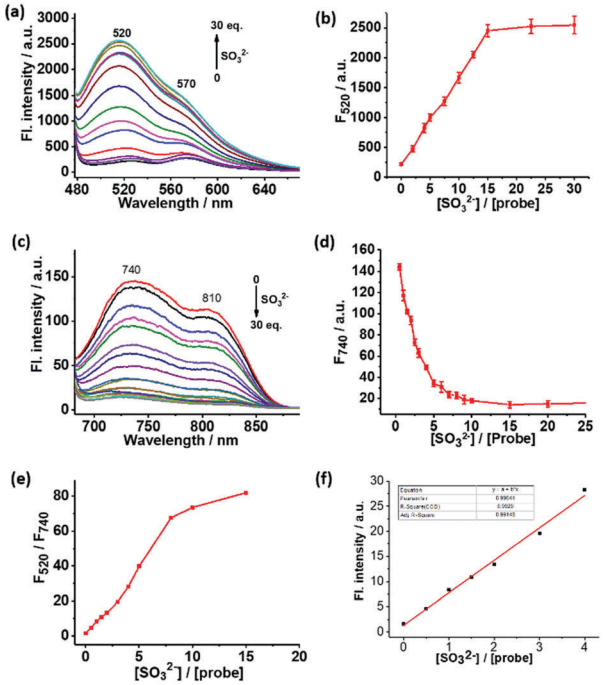

Fig. 3 The fluorescence spectra change of **Rh-TPA** titrated with SO_3^{2-}. (a and c) 10 μM of **Rh-TPA** titrated with increasing amounts of SO_3^{2-} in PBS (pH 7.4, 10 mM, with 10% DMSO as co-solvent), (a) excitation by 440 nm and (c) excitation by 640 nm. (b and d) The fluorescence intensity changes at 520 nm and 640 nm with SO_3^{2-} to probe ratio change (b) monitored at 520 nm and (d) monitored at 740 nm. (e) The ratiometric fluorescence intensity change (F_{520}/F_{740}) with SO_3^{2-} to probe ratio. Error bars are ±SD, n = 3.

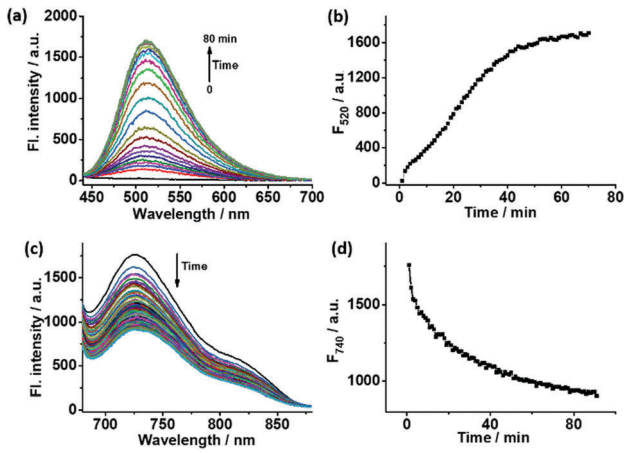

Fig. 4 The time-dependent fluorescence change of **Rh-TPA** in the presence of SO_3^{2-}. (a and c) The fluorescence spectra change of 10 μM of **Rh-TPA** in the presence of 30 equivalents of SO_3^{2-}, (a) and (c) excited at 440 nm and 640 nm, respectively. (b and d) The fluorescence intensity changes at 520 nm and 640 nm with time, respectively.

of the double bond in **Rh-TPA** at 8.04 ppm and 7.65 ppm shifted upfield to 4.89 ppm and 5.76 ppm, respectively. The result was further confirmed by LC-MS analysis (Fig. S6b, ESI†); the prominent peak at m/z of 673.2362 (retention time, 1.80 min) corresponding to the addition product was identified in the HR-MS spectra. The results suggested that sulphite was added to **Rh-TPA** *via* 1,2 conjugated addition, which has been demonstrated in previous reports.[25,26]

The selectivity of probe Rh-TPA towards SO_2 derivative

Among all the factors of a probe for small molecule detection, the selectivity of a probe is one of the key fundamental parameters because of the complexity of biological samples. Thus, the fluorescence responses of **Rh-TPA** towards other reactive species including reactive oxygen species (H_2O_2, ClO^-, TBHP, $^{\bullet}OH$), reactive nitrogen species (NO, HNO, NO_2^-, NO_3^-), reactive sulfur species (H_2S, $S_2O_3^{2-}$, SO_4^{2-}, Cys, Hcy, GSH) and other traditional small molecule species in the physiological environment were also measured. Fig. 5(a–c) demonstrate that **Rh-TPA** exhibited excellent selectivity toward SO_3^{2-}, and other traditional small molecules almost caused negligible interference to the detection process. Moreover, detection could be achieved with multiple fluorescence changes at both 520 nm and 740 nm, and the ratio change of the fluorescence signals (F_{520}/F_{740}) greatly enhanced the detection sensitivity. Peroxy nitrite ($ONOO^-$) is an important species with strong oxidizing ability.[32] The fluorescence change of **Rh-TPA** toward $ONOO^-$ was also measured (Fig. S7, ESI†); the result indicated that it exhibited no fluorescence interference to the detection of sulphite derivatives.

Detection of SO_2 in living cells

With the above measured properties for SO_2 derivative detection in solution, the potential application of **Rh-TPA** for fluorescence imaging of SO_2 derivatives in biological environment was explored. First, we performed an MTT assay to evaluate the cytotoxicity of **Rh-TPA** toward HeLa cells. The results showed that more than 90% of cells survived even after 20 μM of **Rh-TPA**

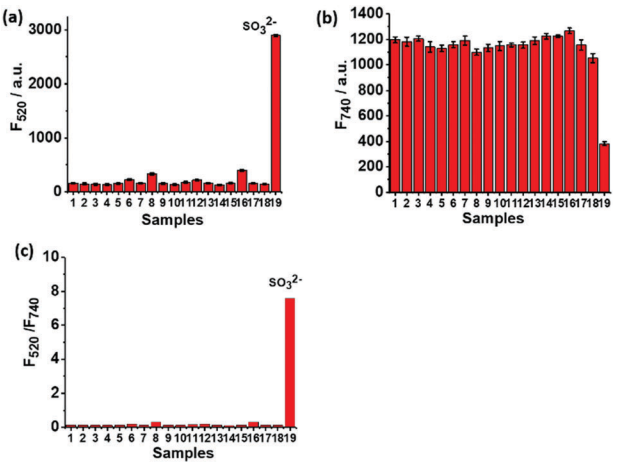

Fig. 5 The selectivity experiment of **Rh-TPA** in the presence of various kinds of species. (a and b) The bar graph of fluorescence intensity changes of 10 μM of **Rh-TPA** in the presence of 30 equivalents of various kinds of species; numbers **1–19** represent blank, Ca^{2+}, Mg^{2+}, Zn^{2+}, Br^-, Cl^-, Ac^-, H_2O_2, ClO^-, $^{\bullet}OH$, GSH, Hcy, Cys, NO_2^-, NO_3^-, NO, $S_2O_3^{2-}$, S^{2-}, SO_3^{2-}. The fluorescence intensity was monitored at 520 nm (a) and 740 nm (b). (c) The ratio changes of fluorescence at 520 nm and 740 nm (F_{520}/F_{740}). Error bars are ±SD, n = 3.

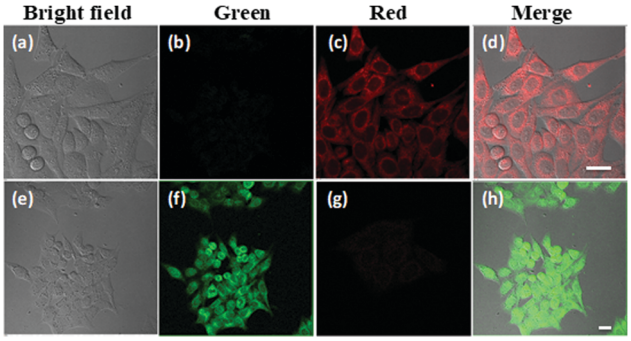

Fig. 6 The confocal fluorescence images of SO_2 derivatives in HeLa cells. (a–d) HeLa cells were incubated with 10 μM of **Rh-TPA** for 20 min; (a) bright field, (b) green channel, (c) red channel, (d) merge. (e–h) HeLa cells were preincubated with SO_2 derivatives for 20 min and then incubated with **Rh-TPA** for 20 min before fluorescence imaging; (e) bright field, (f) green channel, (g) red channel, (h) merge. Red channel: λ_{ex} = 640 nm, filter: 750 ± 20 nm; green channel: λ_{ex} = 488 nm, filter: 550 ± 20 nm. Scale bar: 20 μm.

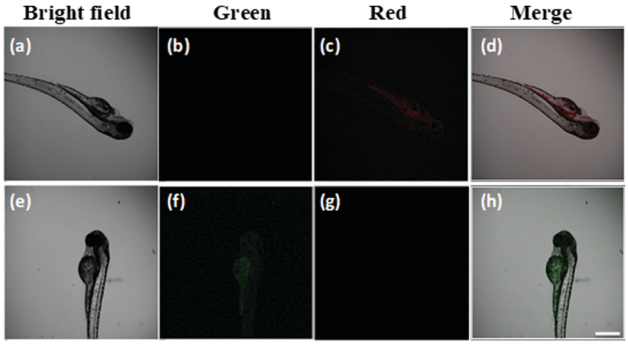

Fig. 7 The confocal fluorescence images of SO_2 derivatives in zebrafish. (a–d) Zebrafish were incubated with 20 μM of **Rh-TPA** for 30 min; (a) bright field, (b) green channel, (c) red channel, (d) merge. (e–h) Zebrafish were preincubated with SO_2 derivatives for 20 min and then incubated with 20 μM of **Rh-TPA** for 30 min before fluorescence imaging; (e) bright field, (f) green channel, (g) red channel, (h) merge. Scale bar: 500 μm.

was internalized for 24 h (Fig. S8, ESI†), suggesting that it has relatively low cytotoxicity and can be applied to image SO_2 derivatives in living cells. We then investigated cell imaging properties toward SO_2 derivatives in HeLa cells (Fig. 6). In the experimental group, HeLa cells were pre-incubated with 50 μM of SO_2 derivatives for 20 min and then incubated with 10 μM of **Rh-TPA** for 20 min. In the control group, HeLa cells were only incubated with 10 μM of **Rh-TPA** for 20 min at 37 °C in an incubator before fluorescence imaging measurements. As expected, in the control group, fluorescence signal was observed only in the red channel (Fig. 6a–d). However, in the experimental group, the fluorescence in the red channel decreased dramatically, and considerable fluorescence enhancement was observed in the green channel synchronously (Fig. 6e–h). Therefore, **Rh-TPA** can detect SO_2 successfully with clear fluorescence signal change in both red and green channels. The fluorescence change was also observed by flow cytometry studies (Fig. S9, ESI†). Compared with the observations for cells incubated with the probe only (Fig. S9c and d, ESI†), the fluorescence in the red channel in the cells incubated with the probe decreased when SO_3^{2-} was added, whereas the fluorescence increased in the green channel under the same conditions (Fig. S9e and f, ESI†).

Furthermore, **Rh-TPA** was applied for detecting endogenous SO_2 in living cells. *N*-Benzyl-2,4-dinitrobenzenesulfonamide was synthesized (Scheme S1, ESI†) and used as an intracellular SO_2 generator.[7,25] As shown in Fig. S10 (ESI†), when the cells were treated with **Rh-TPA**, a bright fluorescence signal was observed in the red channel (Fig. S10a–d, ESI†). However, in the cells pretreated with an SO_2 donor and then incubated with **Rh-TPA**, the fluorescence in the red channel diminished; meanwhile, the fluorescence in the green channel increased sharply (Fig. S10e–h, ESI†). The results indicated that the probe can be used for detecting endogenously generated SO_2 in cells effectively.

Detection of SO_2 derivatives *in vivo*

With the probe in hand, we then explored the ability for SO_2 detection in living animals. Zebrafish is a typical vertebrate animal model widely used in pharmaceutical and biological research.[33] Herein, we investigated the fluorescence detection of SO_2 in zebrafish by **Rh-TPA**. Four-day-old zebrafish were used in the experiments (Fig. 7). In the experimental group, zebrafish were preincubated with an SO_2 derivative for 30 min and then further incubated with 20 μM of **Rh-TPA** for another 30 min. In the control group, zebrafish were incubated with 20 μM of **Rh-TPA** only before fluorescence imaging. As shown in Fig. 7(a–d), a fluorescence signal was observed in the red channel in the zebrafish incubated with the probe only. However, in the experimental group, bright fluorescence increase was observed in the green channel and the fluorescence signal in the red channel diminished sharply (Fig. 7e–h). The experimental results indicated that **Rh-TPA** can potentially be used as an efficient probe for SO_2 derivative detection in living animals.

Conclusions

In summary, we have constructed a novel near-infrared fluorescent probe for SO_2 derivatives with multiple fluorescence emission by incorporating triphenylamine group in **Rh-TPA**. The probe showed near infrared fluorescence emission peaks at 740 nm and 810 nm; after interacting with SO_2 derivatives, two emission peaks emerged in the visible light region. The probe could detect SO_2 derivatives with both colorimetric and ratiometric characteristics and excellent selectivity in solution. As indicated by biological experiments, **Rh-TPA** could detect SO_2 derivatives efficiently in HeLa cells and zebrafish with remarkable fluorescence changes in both red and green channels. As indicated by the photophysical and biological experiments, the probe exhibited excellent near infrared emission properties and good biocompatibility; thus, it can potentially be applied as a novel unit in many fields such as organic photovoltaic materials, optical materials and drug delivery areas in the future.

Conflicts of interest

There are no conflicts to declare.

Acknowledgements

This work was financially supported by NSFC (61605060, 31600472, 31570566, and 31500489), Natural Science Foundation of Shandong Province (ZR2017LEM009), the Foundation of Key Laboratory of Pulp and Paper Science and Technology of Ministry of Education/Shandong Province of China (No. ZR201707 and ZR201710), the Key Research and Development Program of Shandong Province (No. 2017GSF17130), the Foundation of Guangxi Key Laboratory of Clean Pulp & Papermaking and Pollution Control of China (KF201717), and the Undergraduate Innovation and Entrepreneurship Program.

Notes and references

1 C. van Thriel, M. Schäper, S. Kleinbeck, E. Kiesswetter, M. Blaszkewicz, K. Golka, E. Nies, M. Raulf-Heimsoth and T. Brüning, *Toxicol. Lett.*, 2010, **196**, 42–50.
2 A. Song, Q. Liao, J. Li, F. Lin, E. Liu, X. Jiang and L. Deng, *Toxicol. Lett.*, 2012, **214**, 320–327.
3 H. Gong, P. A. Lachenbruch, P. Harber and W. S. Linn, *Toxicol. Ind. Health*, 1995, **11**, 467–487.
4 D. Liu, H. Jin, C. Tang and J. Du, *Mini-Rev. Med. Chem.*, 2010, **10**, 1039–1045.
5 X.-B. Wang, J.-B. Du and H. Cui, *Life Sci.*, 2014, **98**, 63–67.
6 Y.-Q. Sun, J. Liu, J. Zhang, T. Yang and W. Guo, *Chem. Commun.*, 2013, **49**, 2637–2639.
7 W. Xu, C. L. Teoh, J. Peng, D. Su, L. Yuan and Y.-T. Chang, *Biomaterials*, 2015, **56**, 1–9.
8 J. Yang, K. Li, J.-T. Hou, L.-L. Li, C.-Y. Lu, Y.-M. Xie, X. Wang and X.-Q. Yu, *ACS Sens.*, 2016, **1**, 166–172.
9 N. L. W. Septiani, Y. V. Kaneti, B. Yuliarto, Nugraha, H. K. Dipojono, T. Takei, J. You and Y. Yamauchi, *Sens. Actuators, B*, 2018, **261**, 241–251.
10 Y. Liu, X. Xu, Y. Chen, Y. Zhang, X. Gao, P. Xu, X. Li, J. Fang and W. Wen, *Sens. Actuators, B*, 2018, **262**, 26–34.
11 J. Li, W. Xie, R. Shao, X. Ju and H. Li, *Sens. Actuators, B*, 2018, **262**, 282–288.
12 M. B. Gerdroodbary, D. D. Ganji, I. Shiryanpour and R. Moradi, *J. Nat. Gas Sci. Eng.*, 2018, **53**, 317–328.
13 V. Chernikova, O. Yassine, O. Shekhah, M. Eddaoudi and K. N. Salama, *J. Mater. Chem. A*, 2018, **6**, 5550–5554.
14 X. Xu, Z. Du, Y. Wang, X. Mao, L. Jiang, J. Yang and S. Hou, *J. Electroanal. Chem.*, 2018, **815**, 220–224.
15 D. Li, H. Duan, Y. Ma and W. Deng, *Anal. Chem.*, 2018, **90**, 5719–5727.
16 L. Yuan, W. Lin, K. Zheng, L. He and W. Huang, *Chem. Soc. Rev.*, 2013, **42**, 622–661.
17 J. Du, M. Hu, J. Fan and X. Peng, *Chem. Soc. Rev.*, 2012, **41**, 4511–4535.
18 (*a*) Y. Yang, Q. Zhao, W. Feng and F. Li, *Chem. Rev.*, 2012, **113**, 192–270; (*b*) Q. Zhao, C. Huang and F. Li, *Chem. Soc. Rev.*, 2011, **40**, 2508–2524; (*c*) Y. Wen, K. Liu, H. Yang, Y. Liu, L. Chen, Z. Liu, C. Huang and T. Yi, *Anal. Chem.*, 2015, **87**, 10579–10584; (*d*) X. Cao, Y. Wu, K. Liu, X. Yu, B. Wu, H. Wu, Z. Gong and T. Yi, *J. Mater. Chem.*, 2012, **22**, 2650–2657.
19 X. Zhou, S. Lee, Z. Xu and J. Yoon, *Chem. Rev.*, 2015, **115**, 7944–8000.
20 H. Zhang, S. Xue and G. Feng, *Sens. Actuators, B*, 2016, **231**, 752–758.
21 B. Roubinet, L. Bailly, E. Petit, P.-Y. Renard and A. Romieu, *Tetrahedron Lett.*, 2015, **56**, 1015–1019.
22 W.-L. Wu, Z.-Y. Wang, X. Dai, J.-Y. Miao and B.-X. Zhao, *Sci. Rep.*, 2016, **6**, 25315.
23 J. Yang, K. Li, J.-T. Hou, C.-Y. Lu, L.-L. Li, K.-K. Yu and X.-Q. Yu, *Sci. China: Chem.*, 2017, **60**, 793–798.
24 S. Kobayashi, M. Tsuzuki and N. Sato, *Plant Cell Physiol.*, 2015, **56**, 1521–1532.
25 Y. Liu, K. Li, M.-Y. Wu, Y.-H. Liu, Y.-M. Xie and X.-Q. Yu, *Chem. Commun.*, 2015, **51**, 10236–10239.
26 (*a*) L.-J. Zhang, Z.-Y. Wang, X.-J. Cao, J.-T. Liu and B.-X. Zhao, *Sens. Actuators, B*, 2016, **236**, 741–748; (*b*) D.-P. Li, Z.-Y. Wang, X.-J. Cao, J. Cui, X. Wang, H.-Z. Cui, J.-Y. Miao and B.-X. Zhao, *Chem. Commun.*, 2016, **52**, 2760–2763; (*c*) G.-J. Song, J. Luo, X.-j. Xing, H.-L. Ma, D. Yang, X.-Q. Cao, Y.-q. Ge and B.-X. Zhao, *New J. Chem.*, 2018, **42**, 3063–3068.
27 (*a*) D. Zhang, L. Wenya, K. Chen, J. Cheng, Y. Zhao and Y. Ye, *RSC Adv.*, 2016, **6**, 103905; (*b*) G. Li, Y. Chen, J. Wang, J. Wu, G. Gasser, L. Ji and H. Chao, *Biomaterials*, 2015, **63**, 128–136.
28 (*a*) K. Dou, G. Chen, F. Yu, Z. Sun, G. Li, X. Zhao, L. Chen and J. You, *J. Mater. Chem. B*, 2017, **5**, 8389–8398; (*b*) K. Dou, Q. Fu, G. Chen, F. Yu, Y. Liu, Z. Cao, G. Li, X. Zhao, L. Xia, L. Chen, H. Wang and J. You, *Biomaterials*, 2017, **133**, 82–93.
29 H. M. Kim and B. R. Cho, *Chem. Rev.*, 2015, **115**, 5014–5055.
30 J. Liu, Y.-Q. Sun, P. Wang, J. Zhang and W. Guo, *Analyst*, 2013, **138**, 2654–2660.
31 J. R. Lakowicz, *Principles of Fluorescence Spectroscopy*, ed. J. R. Lakowicz, Springer, 2006, pp. 623–673.
32 (*a*) D. Cheng, Y. Pan, L. Wang, Z. Zeng, L. Yuan, X. Zhang and Y.-T. Chang, *J. Am. Chem. Soc.*, 2017, **139**, 285–292; (*b*) K. Konishi, N. Watanabe and T. Arai, *Nitric oxide*, 2009, **20**, 270–278.
33 M. D. Hammers, M. J. Taormina, M. M. Cerda, L. A. Montoya, D. T. Seidenkranz, R. Parthasarathy and M. D. Pluth, *J. Am. Chem. Soc.*, 2015, **137**, 10216–10223.